Longitudinal wave-breaking limits in a unified geometric model of relativistic warm plasmas

2010 J. Phys. A: Math. Theor. 43 075502

(http://iopscience.iop.org/1751-8121/43/7/075502)

J. Phys. A: Math. Theor. **43** (2010) 075502 (19pp) doi:10.1088/1751-8113/43/7/075502

Longitudinal wave-breaking limits in a unified geometric model of relativistic warm plasmas

D A Burton[1,2] **and A Noble**[1,3]

[1] Department of Physics, Lancaster University, Lancaster LA1 4YB, UK
[2] The Cockcroft Institute, Daresbury WA4 4AD, UK
[3] Department of Physics, University of Strathclyde, Glasgow G4 0NG, UK

E-mail: d.burton@lancaster.ac.uk

Received 8 September 2009, in final form 30 November 2009
Published 1 February 2010
Online at stacks.iop.org/JPhysA/43/075502

Abstract

The covariant Vlasov–Maxwell system is used to study the breaking of relativistic warm plasma waves. The well-known theory of relativistic warm plasmas due to Katsouleas and Mori (KM) is subsumed within a unified geometric formulation of the 'waterbag' paradigm over spacetime. We calculate the maximum amplitude $E_{\max}$ of nonlinear longitudinal electric waves for a particular class of waterbags whose geometry is a simple three-dimensional generalization (in velocity) of the one-dimensional KM waterbag (in velocity). It has been shown previously that the value of $\lim_{v\to c} E_{\max}$ (with the effective temperature of the plasma electrons held fixed) diverges for the KM model; however, we show that a certain class of simple three-dimensional waterbags exhibit a finite value for $\lim_{v\to c} E_{\max}$, where v is the phase velocity of the wave and c is the speed of light.

PACS numbers: 52.27.Ny, 52.35.Mw, 52.65.Ff

1. Introduction

Considerable effort has been devoted to developing compact accelerators employing the enormous electric fields present in plasma wakes driven by intense lasers [1] or charged particle beams [2] (see [3, 4] for recent discussions). Conventional accelerators operate by exciting RF microwave cavities with klystrons and use the longitudinal electric component of a cavity mode to accelerate bunches of charged particles for subsequent collision. However, it is anticipated that electric field strengths in the next generation of accelerators will be so high that the RF cavity walls may undergo electrical breakdown [5]. To address this issue, researchers have turned to plasma-based acceleration mechanisms whose field can be orders of magnitude beyond that of conventional accelerators. Recent years have seen the on-going

development of *compact* sources of intense electromagnetic radiation in the x-ray to THz frequency range [6] that employ laser-driven plasma acceleration. Such sources promise a wide range of applications in medicine, material science and security.

A sufficiently short and intense laser pulse propagating through a plasma may create a travelling longitudinal plasma wave whose velocity is approximately the same as the laser pulse's group velocity. However, it is not possible to sustain arbitrarily large electric fields; substantial numbers of plasma electrons become trapped in the wave and are accelerated, which dampens the wave. Indeed, the trapping phenomenon in longitudinal plasma waves lies at the heart of the original laser wakefield accelerator concept [1].

Although the evolution of a plasma wave dynamically trapping particles is complex, over the years much effort has been devoted to analytically understanding the upper bound ('wave-breaking limit') on the amplitude of plasma waves. Wave-breaking limits were first calculated for cold plasmas [7, 8] undergoing nonlinear longitudinal electrostatic oscillations, and thermal effects were later included in non-relativistic [9] and relativistic [10–12] contexts. The results for the cold plasma are uncontroversial, but recent discussion [13–15] has uncovered difficulties with establishing an agreed analytical description of longitudinal wave-breaking in warm plasmas; in particular, it has been noted that different plasma models based on different assumptions yield different results. Models of nonlinear plasma waves near breaking are approaching the limits of their domain of applicability, and different models exhibit different wave-breaking limits. Although recent experiments [16–18] operate in the three-dimensional 'bubble' (or 'blow-out') regime [19] and exploit *transverse* wave-breaking [20], recent work [13–15] has rekindled interest in the theory of longitudinal wave-breaking.

Recent discussion [13–15] includes comparison of the behaviour of the relativistic 'waterbag' model [10, 21] due to Katsouleas and Mori (KM) and a warm plasma model [12] due to Schroeder, Esarey and Shadwick (SES) employing velocity moments of the one-particle plasma electron distribution. The KM and SES models yield different results for the maximum amplitude of nonlinear electrostatic oscillations in the limit $v \to c$ with the temperature of the plasma held fixed (v is the phase velocity of the plasma wave in the laboratory frame). The KM maximum electric field diverges logarithmically in $\gamma = 1/\sqrt{1 - v^2/c^2}$ as $v \to c$, whereas the SES maximum electric field tends to a finite value as $v \to c$ (with the initial plasma temperature held fixed in the limit $v \to c$). Employing velocity moments of the one-particle plasma electron distribution, SES require that the distribution remains narrow in velocity spread whereas the KM approach employs a particular waterbag solution to the Vlasov equation. Unlike more general distributions, waterbag distributions are piecewise constant in velocity throughout their evolution as determined by the Vlasov equation. The disagreement of the two approaches has been attributed to the waterbag's piecewise constant structure and lack of a tail [14].

The KM model is formulated over two-dimensional spacetime and SES employ a line distribution in longitudinal velocity to simplify their field equations on four-dimensional spacetime. Neither model admits a plasma electron distribution with a non-vanishing *transverse* thermal spread. Thus, a theory of waterbags over four-dimensional spacetime was recently developed [22, 23] to permit analytical investigation of wave-breaking as a function of the three-dimensional shape (in velocity) of the plasma electron distribution. In the following, we cast the KM field equations in a form comparable with those of waterbags over four-dimensional spacetime and, for the first time, give a unified presentation of the derivation of wave-breaking limits in the KM model and our waterbag model. We conclude with a comparison of the predictions of a particular class of our waterbags, the KM model and SES model. We find that the results of our present approach have more in common with the SES model than the KM model.

2. Vlasov–Maxwell equations

The brief summary of the Vlasov–Maxwell equations given below establishes our conventions; further details may be found in [23, 24]. We employ the Einstein summation convention throughout this paper. Latin indices a, b, c run over 0, 1, 2, 3 and units are used in which the speed of light $c = 1$ and the permittivity of the vacuum $\varepsilon_0 = 1$.

Let (x^a) be an inertial coordinate system on Minkowski spacetime $(\mathcal{M}, g)$ where x^0 is the proper time of observers at fixed Cartesian coordinates (x^1, x^2, x^3) in the laboratory. The metric tensor g has the form

$$g = \eta_{ab}\, \mathrm{d}x^a \otimes \mathrm{d}x^b \tag{1}$$

where

$$\eta_{ab} = \begin{cases} -1 & \text{if} \quad a = b = 0, \\ 1 & \text{if} \quad a = b \neq 0, \\ 0 & \text{if} \quad a \neq b. \end{cases} \tag{2}$$

Let $(x^a, \dot{x}^b)$ be an induced coordinate system on the total space $T\mathcal{M}$ of the tangent bundle $(T\mathcal{M}, \Pi, \mathcal{M})$, and in the following, where convenient, we will write x instead of x^a and $\dot{x}$ instead of $\dot{x}^b$. For notational simplicity, we will not distinguish between a point in a manifold and its coordinate representation.

The total space $\mathcal{E}$ of the sub-bundle $(\mathcal{E}, \Pi|_{\mathcal{E}}, \mathcal{M})$ of $(T\mathcal{M}, \Pi, \mathcal{M})$ is the set of timelike, future-directed, unit normalized tangent vectors on $\mathcal{M}$:

$$\mathcal{E} = \{(x, \dot{x}) \in T\mathcal{M} \mid \varphi = 0 \text{ and } \dot{x}^0 > 0\}, \tag{3}$$

where

$$\varphi = \eta_{ab}\, \dot{x}^a \dot{x}^b + 1. \tag{4}$$

Plasma electrons are described statistically by a one-particle distribution f on $T\mathcal{M}$ which induces a number 4-current vector field N,

$$N = N^a \frac{\partial}{\partial x^a}, \tag{5}$$

$$N^a(x) = \int_{\mathcal{E}_x} \dot{x}^a f\, \iota_X \#1, \tag{6}$$

where $\mathcal{E}_x = (\Pi|_{\mathcal{E}})^{-1}(x)$ is the fibre of $(\mathcal{E}, \Pi|_{\mathcal{E}}, \mathcal{M})$ over $x \in \mathcal{M}$. The 3-form $\iota_X \#1$ on $T\mathcal{M}$ is induced from the 4-form $\#1$,

$$\#1 = \mathrm{d}\dot{x}^0 \wedge \mathrm{d}\dot{x}^1 \wedge \mathrm{d}\dot{x}^2 \wedge \mathrm{d}\dot{x}^3, \tag{7}$$

and the dilation vector field X,

$$X = \dot{x}^a \frac{\partial}{\partial \dot{x}^a}, \tag{8}$$

on $T\mathcal{M}$, where ι_X is the interior product on forms. It may be shown

$$\iota_X \#1 \simeq \frac{1}{\sqrt{1 + |\dot{\boldsymbol{x}}|^2}}\, \mathrm{d}\dot{x}^1 \wedge \mathrm{d}\dot{x}^2 \wedge \mathrm{d}\dot{x}^3, \tag{9}$$

where $|\dot{\boldsymbol{x}}|^2 = (\dot{x}^1)^2 + (\dot{x}^2)^2 + (\dot{x}^3)^2$ and $\simeq$ denotes equality under restriction to $\mathcal{E}$ by pull- back. The above are specialised to inertial coordinates (x^a) on Minkowski spacetime; their form in a general coordinate system may be found in [23, 24].

We are interested in the evolution of a plasma over timescales during which the motion of the ions is negligible in comparison with the motion of the electrons. We assume that the ions are at rest and distributed homogeneously in the laboratory frame. Their worldlines are trajectories of the vector field $N_{\text{ion}} = n_{\text{ion}}\partial/\partial x^0$ on $\mathcal{M}$ where n_{ion} is the ion number density (a positive constant) in the laboratory frame. The Maxwell equations are

$$dF = 0, \tag{10}$$

$$d \star F = -q \star \widetilde{N} + q \star \widetilde{N_{\text{ion}}}, \tag{11}$$

where $F = \frac{1}{2} F_{ab}\, \mathrm{d}x^a \wedge \mathrm{d}x^b$ is the electromagnetic 2-form and q is the charge on the electron (with $q < 0$). The Hodge map $\star$ is induced from (1) and the volume 4-form $\star 1$,

$$\star\, 1 = \mathrm{d}x^0 \wedge \mathrm{d}x^1 \wedge \mathrm{d}x^2 \wedge \mathrm{d}x^3, \tag{12}$$

on $\mathcal{M}$ and $\star$ satisfies the identity

$$\star\, (\beta \wedge \widetilde{Y}) = \iota_Y \star \beta \tag{13}$$

for all p-forms β and vector fields Y on $\mathcal{M}$. The 1-forms $\widetilde{N}$, $\widetilde{N_{\text{ion}}}$ are the metric duals of the vector fields N, N_{ion}, respectively, i.e. the 1-form $\widetilde{Y}$ satisfies $\widetilde{Y}(Z) = g(Y, Z)$ for all vector fields Z on $\mathcal{M}$.

The scalar field f satisfies the Vlasov equation, which may be written as

$$\dot{x}^a \left(\frac{\partial f}{\partial x^a} - \frac{q}{m} F^{b\mathbf{V}}{}_a \frac{\partial f}{\partial \dot{x}^b} \right) \simeq 0 \tag{14}$$

on $\mathcal{E}$, where $F^{b\mathbf{V}}_{\ a}$ is the vertical lift of $F^b{}_a = \eta^{bc} F_{ca}$ from $\mathcal{M}$ to $T\mathcal{M}$,

$$F^{b\mathbf{V}}_{\ a}(x, \dot{x}) = F^b{}_a(x), \tag{15}$$

and m is the electron rest mass.

The equations of motion for a waterbag distribution are readily motivated via a global expression of the local Vlasov equation (14). Introduce the Liouville vector field L,

$$L = \dot{x}^a \left(\frac{\partial}{\partial x^a} - \frac{q}{m} F^{b\mathbf{V}}{}_a \frac{\partial}{\partial \dot{x}^b} \right), \tag{16}$$

on $T\mathcal{M}$ and the 6-form ω,

$$\omega = \iota_L\, \iota_X (\star 1^{\mathbf{V}} \wedge \#1) \tag{17}$$

where the 4-form $\star 1^{\mathbf{V}}$,

$$\star\, 1^{\mathbf{V}} = \mathrm{d}x^0 \wedge \mathrm{d}x^1 \wedge \mathrm{d}x^2 \wedge \mathrm{d}x^3, \tag{18}$$

is the vertical lift of the spacetime volume 4-form $\star 1$ from $\mathcal{M}$ to $T\mathcal{M}$. It can be shown

$$\mathrm{d}\omega \simeq 0 \tag{19}$$

and the Vlasov equation (14) can be written as

$$\mathrm{d}(f\omega) \simeq 0. \tag{20}$$

Thus, it follows

$$\int_{\mathcal{B}} \mathrm{d}(f\omega) = 0, \tag{21}$$

where $\mathcal{B}$ is a seven-dimensional region in $\mathcal{E}$ and using Stokes' theorem on forms (see, for example, [25, 26]), we obtain

$$\int_{\partial\mathcal{B}} f\omega = 0, \tag{22}$$

where $\partial\mathcal{B}$ is the boundary of $\mathcal{B}$.

2.1. Waterbag distributions

We consider distributions for which $f = \alpha$ is a positive constant inside a seven-dimensional region $\mathcal{U} \subset \mathcal{E}$ and $f = 0$ outside. In particular, we consider $\mathcal{U}$ to be the union over each point $x \in \mathcal{M}$ of a domain $\mathcal{W}_x$ whose boundary $\partial\mathcal{W}_x$ in $\mathcal{E}_x$ is topologically equivalent to the 2-sphere. Such piecewise constant distributions are called 'waterbags'.

Choosing $\mathcal{B}$ in (22) to be a small seven-dimensional 'pill-box' that intersects $\partial\mathcal{W}_x$ and evaluating the integral in the limit as the 'height' of $\mathcal{B}$ tends to zero, we recover a jump condition on $f\omega$ that leads to

$$d\lambda \wedge \omega \simeq 0 \ \text{ at } \lambda = 0, \tag{23}$$

where $\lambda = 0$ is the union over x of the boundaries $\partial\mathcal{W}_x$. If $\lambda = 0$ is the image of the embedding map Σ,

$$\Sigma : \mathcal{M} \times S^2 \to \mathcal{E} \tag{24}$$

$$(x, \xi) \mapsto (x, \dot{x} = V_\xi(x)), \tag{25}$$

where $\xi \in S^2$ has coordinates (ξ^1, ξ^2), then it follows [23] from (8), (16) and (17) that (23) is equivalent to

$$\left(\nabla_{V_\xi} \widetilde{V}_\xi - \frac{q}{m} \iota_{V_\xi} F\right) \wedge \Omega_\xi = 0. \tag{26}$$

Here, V_ξ and Ω_ξ are families of vector fields and 2-forms on $\mathcal{M}$ respectively, where

$$V_\xi = V_\xi^a \frac{\partial}{\partial x^a}, \tag{27}$$

$$\Omega_\xi = \frac{\partial V_\xi^a}{\partial \xi^1} \, \mathrm{d}x_a \wedge \frac{\partial V_\xi^b}{\partial \xi^2} \, \mathrm{d}x_b, \tag{28}$$

with $\mathrm{d}x_a = \eta_{ab} \, \mathrm{d}x^b$ and ∇ the Levi-Civita connection on $\mathcal{M}$. Since the image of Σ lies in $\mathcal{E}$, it follows that, for each $\xi \in S^2$, V_ξ is timelike, unit normalized and future-directed:

$$g(V_\xi, V_\xi) = -1, \qquad g\left(V_\xi, \frac{\partial}{\partial x^0}\right) < 0. \tag{29}$$

We adopt (26) as the equation of motion for the waterbag boundary $\partial\mathcal{W}_x$.

Since $g(V_\xi, V_\xi)$ is constant, it follows $\nabla_{V_\xi} \widetilde{V}_\xi = \iota_{V_\xi} \, \mathrm{d}\widetilde{V}_\xi$, and a particular class of solutions to (26) satisfies

$$F = \frac{m}{q} \, \mathrm{d}\widetilde{V}_\xi. \tag{30}$$

Using (11) and (30), we obtain the field equation

$$d \star \mathrm{d}\widetilde{V}_\xi = -\frac{q^2}{m}(\star\widetilde{N} - \star\widetilde{N_{\mathrm{ion}}}) \tag{31}$$

on $\mathcal{M}$ with the condition that $\mathrm{d}\widetilde{V}_\xi$ is independent of ξ. For simplicity, we have neglected the direct contribution of the driver (laser pulse or particle bunch) to the total electromagnetic field in (30).

For a discussion of solutions to (26) that do not satisfy (30), see [23].

3. Electrostatic oscillations on two-dimensional spacetime

Before analysing (29) and (31) further it is useful to briefly discuss their analogue on two-dimensional spacetime for facilitating comparison with the approach adopted in [10, 21].

Although formulated on four-dimensional spacetime, equations (29) and (31) have a similar structure for any number of dimensions. In particular, we now consider two-dimensional Minkowski spacetime $(\mathcal{M}_2, g)$,

$$g = -\mathrm{d}t \otimes \mathrm{d}t + \mathrm{d}z \otimes \mathrm{d}z, \tag{32}$$

$$\star 1 = \mathrm{d}t \wedge \mathrm{d}z, \tag{33}$$

where (t, z)[4] is a Cartesian coordinate system in the laboratory inertial frame. An induced coordinate system on $T\mathcal{M}_2$ is $(t, z, \dot{t}, \dot{z})$, and the 2-form #1 and dilation vector field X over $T\mathcal{M}_2$ are

$$\#1 = \mathrm{d}\dot{t} \wedge \mathrm{d}\dot{z}, \tag{34}$$

$$X = \dot{t}\frac{\partial}{\partial \dot{t}} + \dot{z}\frac{\partial}{\partial \dot{z}}. \tag{35}$$

Furthermore, ξ is now an element of the 0-sphere $\{+, -\}$ and $\Omega_\xi = 1$ is a constant 0-form. Thus, the analogue to (26) is

$$\nabla_{V_+}\widetilde{V_+} - \frac{q}{m}\iota_{V_+}F = 0, \tag{36}$$

$$\nabla_{V_-}\widetilde{V_-} - \frac{q}{m}\iota_{V_-}F = 0, \tag{37}$$

where $\{V_+, V_-\}$ satisfy the conditions

$$g(V_+, V_+) = -1, \qquad g\left(V_+, \frac{\partial}{\partial t}\right) < 0, \tag{38}$$

$$g(V_-, V_-) = -1, \qquad g\left(V_-, \frac{\partial}{\partial t}\right) < 0, \tag{39}$$

and the only non-trivial Maxwell equation for the 2-form F is

$$d \star F = -q \star \widetilde{N} + q \star \widetilde{N_{\mathrm{ion}}}, \tag{40}$$

where $N_{\mathrm{ion}} = n_{\mathrm{ion}}\partial/\partial t$ is the ion number 2-current and $F = E\,\mathrm{d}t \wedge \mathrm{d}z$ where E is the electric field along the z-axis. As noted previously, we assume n_{ion} is constant.

On the unit hyperbola bundle $\mathcal{E}_2$, $\dot{t} = \sqrt{1 + \dot{z}^2}$ and the components of the electron number 2-current $N = N^t\partial/\partial t + N^z\partial/\partial z$ corresponding to (6) are

$$N^t = \int_{\mathbb{R}} f(t, z, \dot{t}, \dot{z})\,\mathrm{d}\dot{z} = \alpha(Y_+ - Y_-), \tag{41}$$

$$N^z = \int_{\mathbb{R}} \frac{\dot{z}}{\sqrt{1 + \dot{z}^2}} f(t, z, \dot{t}, \dot{z})\,\mathrm{d}\dot{z} = \alpha\left(\sqrt{1 + Y_+^2} - \sqrt{1 + Y_-^2}\right), \tag{42}$$

where

$$f = \begin{cases} \alpha, & Y_- \leqslant \dot{z} \leqslant Y_+, \\ 0, & \dot{z} < Y_- \text{ or } \dot{z} > Y_+ \end{cases} \tag{43}$$

[4] We use (t, z) rather than (x^a) to distinguish coordinates on two- and four-dimensional spacetimes.

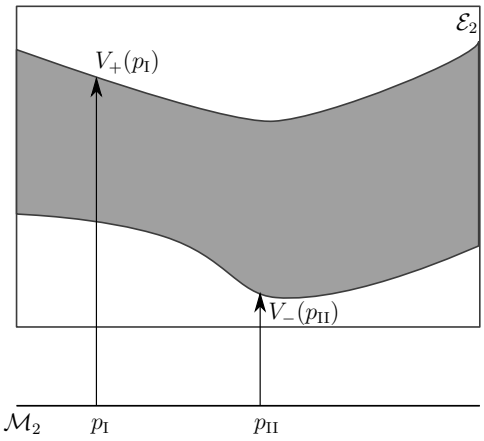

Figure 1. Illustration of a waterbag distribution over two-dimensional spacetime $\mathcal{M}_2$ with $p_\mathrm{I} = (t_\mathrm{I}, z_\mathrm{I})$ and $p_\mathrm{II} = (t_\mathrm{II}, z_\mathrm{II})$. The shaded region is the interior of the waterbag (where f is non-zero), and the 2-vector fields $\{V_+, V_-\}$ determine the boundary of the waterbag.

with α a positive constant and $\{Y_+, Y_-\}$ 0-forms on $\mathcal{M}_2$. The 2-velocity fields $\{V_+, V_-\}$ satisfy

$$V_\pm = \sqrt{1 + Y_\pm^2}\,\frac{\partial}{\partial t} + Y_\pm \frac{\partial}{\partial z} \tag{44}$$

and it follows

$$\widetilde{N} = \alpha\star(\widetilde{V_+} - \widetilde{V_-}). \tag{45}$$

See figure 1.

Unlike their four-dimensional analogue, which may include transverse electromagnetic fields, (36) and (37) are *uniquely*[5] solved by

$$\mathrm{d}\widetilde{V_\pm} = \frac{q}{m}F, \tag{46}$$

and using (40) it follows

$$d\star\,\mathrm{d}\widetilde{V_\pm} = -\frac{q^2}{m}(\star\widetilde{N} - \star\widetilde{N_\mathrm{ion}}) \tag{47}$$

subject to the condition $\mathrm{d}\widetilde{V_+} = \mathrm{d}\widetilde{V_-}$.

Alternatively, one may follow the approach adopted in [10] by casting the above as a warm fluid. The type (0, 2) stress–energy–momentum tensor $\mathcal{T}_\mathrm{fluid}$ of the electron fluid is

$$\mathcal{T}_\mathrm{fluid} = \left(m\int_{\mathbb{R}} \frac{\dot{z}^\mu \dot{z}^\nu f}{\sqrt{1+\dot{z}^2}}\,\mathrm{d}\dot{z}\right)\frac{\partial}{\partial z^\mu}\otimes\frac{\partial}{\partial z^\nu}, \tag{48}$$

where Greek indices μ, ν run over 0, 1 and $z^0 = t$, $z^1 = z$, $\dot{z}^0 = \sqrt{1+\dot{z}^2}$, $\dot{z}^1 = \dot{z}$. It can be shown that $\mathcal{T}_\mathrm{fluid}$ induced by the above waterbag distribution can be expressed entirely in terms of the proper number density n of the electron fluid, the electron fluid's bulk 2-velocity U and the spacetime metric:

$$\mathcal{T}_\mathrm{fluid} = (\rho + p)U\otimes U + p\,\widetilde{g}, \tag{49}$$

[5] Proper incorporation of transverse fields requires at least two spatial dimensions.

where $\widetilde{g}$ is the inverse metric tensor,

$$\tilde{g} = -\frac{\partial}{\partial t} \otimes \frac{\partial}{\partial t} + \frac{\partial}{\partial z} \otimes \frac{\partial}{\partial z} \tag{50}$$

and

$$U = \frac{1}{\sqrt{-g(Z,Z)}} Z, \qquad Z = \frac{1}{2}(V_+ + V_-), \tag{51}$$

$$N = nU, \qquad n = \sqrt{-g(N,N)}, \tag{52}$$

with the equations of state

$$\rho = m\alpha \left[\frac{n}{2\alpha} \sqrt{1 + \left(\frac{n}{2\alpha}\right)^2} + \sinh^{-1}\left(\frac{n}{2\alpha}\right) \right], \tag{53}$$

$$p = m\alpha \left[\frac{n}{2\alpha} \sqrt{1 + \left(\frac{n}{2\alpha}\right)^2} - \sinh^{-1}\left(\frac{n}{2\alpha}\right) \right]. \tag{54}$$

The equation of motion of the electron fluid

$$(\rho + p)\nabla_U \widetilde{U} = qn\iota_U F - \iota_U(\mathrm{d}p \wedge \widetilde{U}), \tag{55}$$

follows from the zero divergence of the sum of $\mathcal{T}_{\text{fluid}}$ and the Maxwell stress–energy–momentum tensor where

$$g(U,U) = -1, \qquad g\left(U, \frac{\partial}{\partial t}\right) < 0. \tag{56}$$

It should be stressed that the warm fluid model (53), (54) and (55) is equivalent to (36), (37), (38) and (39). Thus, (36), (37), (38) and (39) may be replaced by an equivalent field theory expressed in terms of a finite set of moments of f on two-dimensional spacetime. However, the situation is more complicated for waterbags over four-dimensional spacetime where second and higher order moments of f in $\dot{x}$ are not, in general, easily expressible in terms of zeroth and first-order moments of f.

We will now obtain a nonlinear ordinary differential equation describing one-dimensional electrostatic oscillations and determine an expression for the wave-breaking limit of this model. Derivation of wave-breaking limits starting from $\mathcal{T}_{\text{fluid}}$ and the equations of state (53) and (54) may be found in [10, 21]. However, we will work directly with (38), (39), (45) and (47) to facilitate comparison with our model on four-dimensional spacetime.

Let all field components with respect to the laboratory frame $(\mathrm{d}t, \mathrm{d}z)$ be functions of $\zeta = z - vt$ only (the 'quasi-static assumption'), where $0 < v < 1$, and let (e^1, e^2) be the basis,

$$e^1 = v\,\mathrm{d}z - \mathrm{d}t, \qquad e^2 = \mathrm{d}z - v\,\mathrm{d}t, \tag{57}$$

for 1-forms on $\mathcal{M}$. The coframe $(\gamma e^1, \gamma e^2)$ is an orthonormal basis adapted to observers moving at velocity v along z (i.e. observers in the 'wave frame') where $\gamma = (1 - v^2)^{-1/2}$ is the Lorentz factor of such observers relative to the laboratory. So, $\gamma e^2(N_{\text{ion}}) = -\gamma n_{\text{ion}} v$ is the component of the ion number 1-current in the wave frame.

In the basis (e^1, e^2), $\widetilde{V_\pm}$ can be decomposed as

$$\widetilde{V_\pm} = (\mu(\zeta) + A_\pm)e^1 + \psi_\pm(\zeta)e^2, \tag{58}$$

where $\{A_+, A_-\}$ are constant. Note that this is the most general decomposition compatible with equation (46) and the quasi-static assumption.

Solving (38) and (39) for $\psi_\pm^2$ gives

$$\psi_\pm^2 = (\mu + A_\pm)^2 - \gamma^2 \tag{59}$$

and additional physical information is needed to fix the sign of $\psi_\pm$. Here, we demand that all electrons described by the waterbag are travelling slower than the wave, so $\psi_\pm = -\sqrt{(\mu + A_\pm)^2 - \gamma^2}$ and (58) is

$$\widetilde{V_\pm} = (\mu + A_\pm)e^1 - ((\mu + A_\pm)^2 - \gamma^2)^{1/2}e^2. \tag{60}$$

Substituting (58) into equation (46) yields

$$E = \frac{1}{\gamma^2}\frac{m}{q}\frac{\mathrm{d}\mu}{\mathrm{d}\zeta}, \tag{61}$$

and equation (47) yields the nonlinear oscillator equation

$$\frac{1}{\gamma^2}\frac{\mathrm{d}^2\mu}{\mathrm{d}\zeta^2} = -\frac{q^2}{m}\gamma^2 n_{\mathrm{ion}} - \frac{q^2}{m}\alpha[\sqrt{(\mu + A_+)^2 - \gamma^2} - \sqrt{(\mu + A_-)^2 - \gamma^2}] \tag{62}$$

with the algebraic constraint

$$A_+ - A_- = -\frac{n_{\mathrm{ion}}\gamma^2 v}{\alpha} < 0. \tag{63}$$

3.1. Electrostatic wave-breaking

In the wave frame, the relativistic energies of the two ends of the waterbag are $m(\mu + A_+)/\gamma$ and $m(\mu + A_-)/\gamma$, respectively, and since $m(\mu + A_+)/\gamma \geqslant m$, it follows $\mu + A_+ \geqslant \gamma$. Using (63), $\mu + A_- > \mu + A_+$ and hence $\mu + A_+ \geqslant \gamma$ implies $\mu + A_- > \gamma$. Thus, $\mu + A_\pm \geqslant \gamma$ may be reduced to $\mu \geqslant \mu_{\mathrm{wb}}$ where

$$\mu_{\mathrm{wb}} = -A_+ + \gamma. \tag{64}$$

Alternatively, one may arrive at the same conclusion by inspecting the right-hand side of (62) and using $\mu + A_\pm > 0$ (which follows because V_+ and V_- are future-pointing). Thus, there is an upper bound on the amplitude of oscillatory solutions to (62), which leads to an upper bound E_{max} on the magnitude $|E|$ of the electric field E (the 'wave-breaking limit' of this model).

During an oscillation E vanishes when $\mathrm{d}\mu/\mathrm{d}\zeta$ vanishes and $|E|$ is at a maximum when $|\mathrm{d}\mu/\mathrm{d}\zeta|$ is at a maximum (see (61) and note $q < 0$). A maximum of $|\mathrm{d}\mu/\mathrm{d}\zeta|$ occurs at values ζ_0 of ζ where $\mu(\zeta_0)$ equals the oscillator equilibrium μ_{eq}. Furthermore, for the maximum amplitude oscillation $\mathrm{d}\mu/\mathrm{d}\zeta$ vanishes when $\mu = \mu_{\mathrm{wb}}$. An upper bound E_{max} on the magnitude $|E|$ of the electric field is obtained by evaluating the first integral of (62) between $\mu = \mu_{\mathrm{wb}}$ and $\mu = \mu_{\mathrm{eq}}$.

Without loss of generality, we can choose the split between μ and $A_\pm$ such that

$$A_+ = -A_- = -a, \qquad a = \frac{n_{\mathrm{ion}}\gamma^2 v}{2\alpha}. \tag{65}$$

Using (61) and (62), it follows

$$E_{\mathrm{max}}^2 = 2mn_{\mathrm{ion}}\left[-\mu_{\mathrm{eq}} + \mu_{\mathrm{wb}} + \frac{1}{2}\frac{v}{a}\int_{\mu_{\mathrm{wb}}}^{\mu_{\mathrm{eq}}}(\sqrt{[\mu + a]^2 - \gamma^2} - \sqrt{[\mu - a]^2 - \gamma^2})\,\mathrm{d}\mu\right], \tag{66}$$

where μ_{eq} is the equilibrium solution to (62), which satisfies

$$\frac{2a}{v} = \sqrt{(\mu_{\mathrm{eq}} + a)^2 - \gamma^2} - \sqrt{(\mu_{\mathrm{eq}} - a)^2 - \gamma^2}. \tag{67}$$

The constant a is fixed in terms of an effective temperature $T_{\rm eq}$ associated with the oscillator equilibrium $\mu_{\rm eq}$. Noting that $n = n_{\rm ion}$ when the waterbag is in its equilibrium state ($\mu = \mu_{\rm eq}$), and assuming $n_{\rm ion} \ll 2\alpha$ in (54), it follows

$$p_{\rm eq} \approx \frac{m n_{\rm ion}^3}{3(2\alpha)^2}. \tag{68}$$

Introducing $T_{\rm eq}$ via $p_{\rm eq} = n_{\rm ion} k_B T_{\rm eq}$, where k_B is Boltzmann's constant, we find

$$\frac{n_{\rm ion}}{2\alpha} \approx \sqrt{\frac{3k_B T_{\rm eq}}{m}}, \qquad a \approx \gamma^2 v \sqrt{\frac{3k_B T_{\rm eq}}{m}}, \tag{69}$$

where (65) has been used. Hence, $n_{\rm ion} \ll 2\alpha$ means that the thermal energy of the electron fluid in the oscillator equilibrium state is much less than the rest mass-energy of the electron.

The wave-breaking limit $E_{\rm max}$ can be readily analysed for $\gamma \gg 1$ via asymptotic approximation in a small parameter ε,

$$\varepsilon = \frac{\gamma}{a} = \frac{2\alpha}{n_{\rm ion} v} \frac{1}{\gamma}, \tag{70}$$

where (65) has been used. Employing (64), (66) and (67), it follows

$$E_{\rm max}^2 = 2 m n_{\rm ion} a \left[-\hat{\mu}_{\rm eq} + \hat{\mu}_{\rm wb} + \frac{1}{2} v \int_{\hat{\mu}_{\rm wb}}^{\hat{\mu}_{\rm eq}} (\sqrt{[\hat{\mu}+1]^2 - \varepsilon^2} - \sqrt{[\hat{\mu}-1]^2 - \varepsilon^2})\, {\rm d}\hat{\mu} \right], \tag{71}$$

and

$$\tfrac{1}{2} v (\sqrt{[\hat{\mu}_{\rm eq}+1]^2 - \varepsilon^2} - \sqrt{[\hat{\mu}_{\rm eq}-1]^2 - \varepsilon^2}) = 1, \tag{72}$$

$$\hat{\mu}_{\rm wb} = 1 + \varepsilon, \tag{73}$$

where $\hat{\mu} = \mu/a$. To proceed further, we express v in (71) and (72) as a function of ε and a parameter b that characterizes the effective temperature of the oscillator equilibrium distribution. Using (70) it follows

$$v = \frac{1}{\sqrt{1 + \varepsilon^2 b^2}}, \tag{74}$$

where b is

$$b = \frac{n_{\rm ion}}{2\alpha}. \tag{75}$$

The dominant ε dependence (as $\varepsilon \to 0$ with b held fixed) of $E_{\rm max}^2$ arises from the second term in the integrand in (71) and may be extracted by expanding the integrand with respect to ε and integrating each term over $\hat{\mu}$. Since, for $v > \varepsilon > 0$,

$$\sqrt{v^2 - \varepsilon^2} = v - \frac{1}{2}\frac{\varepsilon^2}{v} + \sum_{n=2}^{\infty} c_n \frac{\varepsilon^{2n}}{v^{2n-1}}, \tag{76}$$

where c_n are constants, and inspection of (72) reveals

$$\hat{\mu}_{\rm eq} = h(\varepsilon^2) = h(0) + h'(0)\varepsilon^2 + \mathcal{O}(\varepsilon^4) \qquad (\varepsilon \to 0), \tag{77}$$

we find, for $h(0) > 1$,

$$\begin{aligned} \int_{\hat{\mu}_{\rm wb}}^{\hat{\mu}_{\rm eq}} \sqrt{[\hat{\mu}-1]^2 - \varepsilon^2}\, {\rm d}\hat{\mu} &= \left(\frac{1}{2}[\hat{\mu}-1]^2 - \frac{1}{2}\varepsilon^2 \ln(\hat{\mu}-1) \right) \Bigg|_{\hat{\mu}_{\rm wb}}^{\hat{\mu}_{\rm eq}} \\ &\quad + \sum_{n=2}^{\infty} c_n \frac{1}{2-2n} \left(\frac{\varepsilon^{2n}}{[\hat{\mu}_{\rm eq}-1]^{2n-2}} - \varepsilon^2 \right) \\ &= \frac{1}{2}[\hat{\mu}-1]^2 \Big|_{\hat{\mu}_{\rm wb}}^{\hat{\mu}_{\rm eq}} + \frac{1}{2}\varepsilon^2 \ln(\varepsilon) + \mathcal{O}(\varepsilon^2) \quad (\varepsilon \to 0), \end{aligned} \tag{78}$$

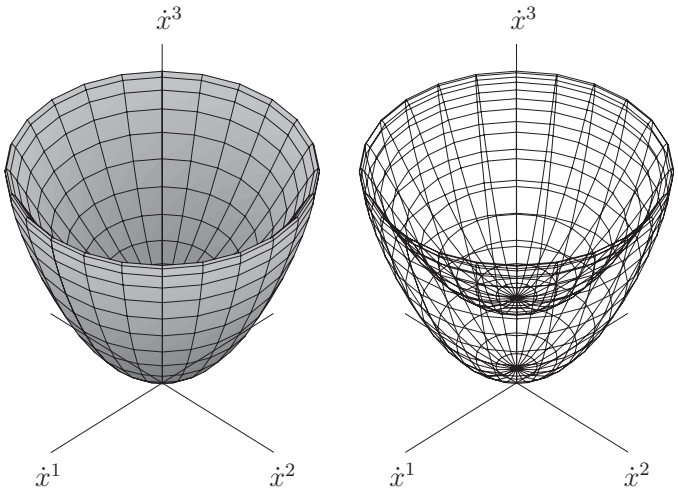

Figure 2. Two illustrations of the 4-velocity dependence of a particular 'bowl' waterbag. The axis of symmetry is aligned along $\dot{x}^3$, and f equals the positive constant α within the 'wall' of the bowl and vanishes outside. The maximum electric field amplitude is achieved during the oscillation in which the top of the waterbag (a circle) grazes the phase speed of the wave.

where (73) has been used. Furthermore, it follows from (72) that an asymptotic approximation for $h(0)$ in small b leads to

$$h(0) = \frac{1}{b} + \mathcal{O}(1) \quad (b \to 0). \tag{79}$$

Thus, (71) yields

$$\frac{E_{\max}^2}{a} \approx -\frac{1}{2} m n_{\text{ion}} \varepsilon^2 \ln(\varepsilon) \tag{80}$$

for $\varepsilon, b \ll 1$. Introducing the effective temperature T_{eq} using (65), (69) and (70) and noting $v \approx 1$ (see (74) with $\varepsilon, b \ll 1$), we obtain

$$E_{\max}^2 \approx \frac{1}{2} \frac{m^2 c^2 \omega_p^2}{q^2} \sqrt{\frac{mc^2}{3k_B T_{\text{eq}}}} \ln\left(\gamma \sqrt{\frac{3k_B T_{\text{eq}}}{mc^2}}\right), \qquad \varepsilon, b \ll 1, \tag{81}$$

where $\omega_p = \sqrt{n_{\text{ion}} q^2/(m\varepsilon_0)}$ is the plasma frequency and the speed of light c and permittivity of the vacuum ε_0 have been restored. Equation (81) was obtained as a lower bound on $E_{\max}^2$ in [13].

4. Longitudinal electrostatic oscillations on four-dimensional spacetime

We now consider longitudinal electrostatic waves on four-dimensional spacetime by closely following the above description on two-dimensional spacetime.

As before, we adopt the 'quasi-static assumption'. We seek a waterbag $\mathcal{W}_x$ axisymmetric about $\dot{x}^3$ whose pointwise dependence in Minkowski spacetime $\mathcal{M}$ is on the wave's phase $\zeta = x^3 - vx^0$ only, where $0 < v < 1$. See figures 2 and 3 for examples of such distributions. As before, the following results are applicable only if the longitudinal component of V_ξ in the wave frame is negative (no electron described by $\mathcal{W}_x$ is moving faster along x^3 than the wave).

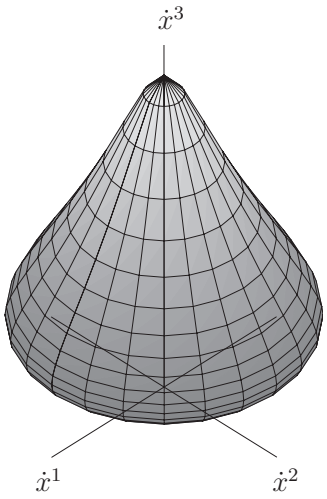

Figure 3. An illustration of the 4-velocity dependence of a particular 'gourd' waterbag. The axis of symmetry is aligned along $\dot{x}^3$, and f equals the positive constant α inside the gourd and vanishes outside. The maximum electric field amplitude is achieved during the oscillation in which the tip of the waterbag grazes the phase speed of the wave.

Decompose $\widetilde{V}_\xi$ in the wave frame as

$$\widetilde{V}_\xi = [\mu(\zeta) + A(\xi^1)]\, e^1 + \psi(\xi^1, \zeta)\, e^2 \; + R\sin(\xi^1)\cos(\xi^2)\,\mathrm{d}x^1 + R\sin(\xi^1)\sin(\xi^2)\,\mathrm{d}x^2 \tag{82}$$

for $0 < \xi^1 < \pi$, $0 \leqslant \xi^2 < 2\pi$ where $R > 0$ is constant and

$$e^1 = v\,\mathrm{d}x^3 - \mathrm{d}x^0, \qquad e^2 = \mathrm{d}x^3 - v\,\mathrm{d}x^0. \tag{83}$$

Here, $(\gamma e^1, \gamma e^2, \mathrm{d}x^1, \mathrm{d}x^2)$ is an orthonormal basis adapted to the wave frame, with $\gamma = 1/\sqrt{1-v^2}$. In the wave frame the relativistic energy of $P_\xi = mV_\xi$ is $m(\mu + A(\xi^1))/\gamma$ and it follows that $\mu + A(\xi^1) > 0$. Furthermore, using (29) and (82) it follows

$$\psi = -\sqrt{[\mu + A(\xi^1)]^2 - \gamma^2[1 + R^2\sin^2(\xi^1)]}, \tag{84}$$

where the negative square root is chosen because no electron is moving faster along x^3 than the wave, and we obtain

$$\mu \geqslant -A(\xi^1) + \gamma\sqrt{1 + R^2\sin^2(\xi^1)}. \tag{85}$$

Each velocity moment $S^{a_1\cdots a_p}$ of f is

$$\begin{aligned} S^{a_1\cdots a_p}(x) &= \int_{\mathcal{E}_x} f(x,\dot{x})\,\dot{x}^{a_1}\cdots\dot{x}^{a_p}\,\iota_X\#1 \\ &= \alpha\int_{\mathcal{W}_x} \dot{x}^{a_1}\cdots\dot{x}^{a_p}\,\iota_X\#1 \\ &= (\hat{S}^{a_1\cdots a_p}\circ\mu)(\zeta), \end{aligned} \tag{86}$$

where the 3-form $\iota_X\#1$ is given in (9), $\dot{x}^{a_1}\cdots\dot{x}^{a_p}$ is a p-fold product of coordinates on $T_x\mathcal{M}$ and $\hat{S}^{a_1\cdots a_p}$ is a function of μ. Although the moment hierarchy associated with (82) is closed, the algebraic relationships between the moments are complicated and it is much simpler to work directly with (31) rather than developing the differential equations satisfied by the moments.

Substituting (82) into equation (30) leads to

$$F = \frac{m}{q}\frac{\mathrm{d}\mu}{\mathrm{d}\zeta} e^2 \wedge e^1, \tag{87}$$

and (6), (31), (82) and (84) yield

$$\frac{1}{\gamma^2}\frac{\mathrm{d}^2\mu}{\mathrm{d}\zeta^2} = -\frac{q^2}{m} n_{\mathrm{ion}} \gamma^2 - \frac{q^2}{m} 2\pi R^2 \alpha \times \int_0^\pi ([\mu + A(\xi^1)]^2 - \gamma^2[1 + R^2 \sin^2(\xi^1)])^{1/2} \sin(\xi^1)\, \cos(\xi^1)\, \mathrm{d}\xi^1 \tag{88}$$

(cf equation (62)) and

$$2\pi R^2 \int_0^\pi A(\xi^1)\, \sin(\xi^1)\, \cos(\xi^1)\, \mathrm{d}\xi^1 = -\frac{n_{\mathrm{ion}} \gamma^2 v}{\alpha} \tag{89}$$

(cf equation (63)) where $\alpha > 0$ is the value of f inside $\mathcal{W}_x$.

The form of the second-order autonomous nonlinear ordinary differential equation (88) for μ is fixed by specifying the generator $A(\xi^1)$ of $\partial\mathcal{W}_x$ subject to the normalization condition (89).

4.1. Electrostatic wave-breaking

The form of the integrand in (88) ensures that the magnitude of oscillatory solutions to (88) cannot be arbitrarily large. For our model, the 'wave-breaking' value μ_{wb} is the largest μ for which the argument of the square root in (88) (i.e. the square ψ^2 of the longitudinal component ψ of $\widetilde{V}_\xi$) vanishes,

$$\mu_{\mathrm{wb}} = \max\left\{-A(\xi^1) + \gamma\sqrt{1 + R^2 \sin^2(\xi^1)} \,\middle|\, 0 \leqslant \xi^1 \leqslant \pi\right\}, \tag{90}$$

because $\mu < \mu_{\mathrm{wb}}$ yields an imaginary integrand in (88) for some ξ^1.

We consider an electric field with only one non-zero component E (in the x^3 direction). Using $F = E\, \mathrm{d}x^0 \wedge \mathrm{d}x^3$ and (83) and (87), it follows

$$E = \frac{m}{q}\frac{1}{\gamma^2}\frac{\mathrm{d}\mu}{\mathrm{d}\zeta} \tag{91}$$

and the wave-breaking limit $E_{\max}$ is obtained by evaluating the first integral of (88) between μ_{wb} where E vanishes and the oscillator equilibrium μ_{eq} of μ where $|E|$ is at a maximum. Using (89) to eliminate α, it follows that μ_{eq} satisfies

$$\frac{1}{v}\int_0^\pi A(\xi^1) \sin(\xi^1) \cos(\xi^1)\, \mathrm{d}\xi^1 = \int_0^\pi ([\mu_{\mathrm{eq}} + A(\xi^1)]^2 - \gamma^2[1 + R^2 \sin^2(\xi^1)])^{1/2} \sin(\xi^1) \cos(\xi^1)\, \mathrm{d}\xi^1 \tag{92}$$

with

$$\int_0^\pi A(\xi^1) \sin(\xi^1) \cos(\xi^1)\, \mathrm{d}\xi^1 < 0 \tag{93}$$

since $\alpha, v > 0$. Equation (88) yields the maximum value $E_{\max}$ of $|E|$,

$$E_{\max}^2 = 2mn_{\mathrm{ion}}\left[-\mu_{\mathrm{eq}} + \mu_{\mathrm{wb}} + \frac{v}{\int_0^\pi A(\xi^{1\prime}) \sin(\xi^{1\prime}) \cos(\xi^{1\prime})\, \mathrm{d}\xi^{1\prime}} \times \int_{\mu_{\mathrm{wb}}}^{\mu_{\mathrm{eq}}} \int_0^\pi ([\mu + A(\xi^1)]^2 - \gamma^2[1 + R^2 \sin^2(\xi^1)])^{1/2} \sin(\xi^1) \cos(\xi^1)\, \mathrm{d}\xi^1\, \mathrm{d}\mu\right]. \tag{94}$$

To proceed further, we need to choose the generator $A(\xi^1)$ of the waterbag distribution. It turns out that even the simple choice

$$A(\xi^1) = -a\cos(\xi^1) \tag{95}$$

for $A(\xi^1)$, where a is a positive constant, leads to a wave-breaking limit $E_{\max}$ with interesting behaviour, as we now show.

Using (94), it follows

$$E_{\max}^2 = 2mn_{\text{ion}}\left[-\mu_{\text{eq}} + \mu_{\text{wb}} + \frac{3}{2}\frac{v}{a}\int_{\mu_{\text{wb}}}^{\mu_{\text{eq}}}\int_{-1}^{1}([\mu + a\chi]^2 - \gamma^2[1 + R^2(1-\chi^2)])^{1/2}\chi\,\mathrm{d}\chi\,\mathrm{d}\mu\right] \tag{96}$$

where $\chi = -\cos(\xi^1)$, and equation (92) yields

$$\frac{3}{2}\frac{v}{a}\int_{-1}^{1}([\mu_{\text{eq}} + a\chi]^2 - \gamma^2[1 + R^2(1-\chi^2)])^{1/2}\chi\,\mathrm{d}\chi = 1 \tag{97}$$

and equation (90) may be written as

$$\mu_{\text{wb}} = \max\left\{-a\chi + \gamma\sqrt{1 + R^2(1-\chi^2)}\;\middle|\; -1 \leqslant \chi \leqslant 1\right\}. \tag{98}$$

Examination of (98) reveals that two classes of waterbag arise according to whether or not the function

$$\chi \mapsto -a\chi + \gamma\sqrt{1 + R^2(1-\chi^2)} \tag{99}$$

has a turning point in the interval $[-1, 1]$. Examples of the two classes are shown in figures 2 and 3. In each case, the plasma wave breaks when the uppermost part of the distribution achieves the phase velocity of the plasma wave (i.e. the longitudinal component ψ of V_ξ in the wave frame vanishes). Wave-breaking limits for the class in figure 2 have been calculated previously [22, 23] and here we focus on waterbags of the type shown in figure 3. Furthermore, a physical bi-Maxwellian distribution has more in common with the oscillator equilibrium (constant μ) configuration of the type of waterbag in figure 3 than that shown in figure 2.

4.1.1. Calculation of the maximum electric field. The parameters a, R, γ are chosen to satisfy

$$\frac{a}{R}\sqrt{\frac{1+R^2}{a^2+\gamma^2R^2}} > 1, \tag{100}$$

ensuring that (99) does not have a turning point in the interval $[-1, 1]$. Hence, the wave breaks when the tip $\chi = -\cos(0) = -1$ of the waterbag achieves the phase velocity of the plasma wave. Using (98), it follows

$$\mu_{\text{wb}} = a + \gamma, \tag{101}$$

which is formally identical to the wave-breaking limit of μ for the waterbag over two-dimensional spacetime. This is quite different from the value of μ_{wb} for waterbags of the type shown in figure 2 (see [22, 23]), where

$$\frac{a}{R}\sqrt{\frac{1+R^2}{a^2+\gamma^2R^2}} < 1. \tag{102}$$

Comparison with the SES model [12] follows by calculating $E_{\max}$ for waterbags whose transverse (i.e. $\dot{x}^1, \dot{x}^2$) extent in $\mathcal{E}_x$ is much smaller than their longitudinal (i.e. $\dot{x}^3$) extent.

Inspection of (102) reveals that the class of waterbag shown in figure 2 does not easily lend itself to this regime.

Following a similar method to that used in section 3, we now evaluate (96) for $\gamma \gg 1$. Introducing $\hat{\mu} = \mu/a$ in (96), (97) and (101) leads to

$$E_{\max}^2 = 2mn_{\text{ion}}a\left[-\hat{\mu}_{\text{eq}} + \hat{\mu}_{\text{wb}} + \frac{3}{2}v\int_{\hat{\mu}_{\text{wb}}}^{\hat{\mu}_{\text{eq}}}\int_{-1}^{1}([\hat{\mu}+\chi]^2 - \varepsilon^2[1+R^2(1-\chi^2)])^{1/2}\chi\,\mathrm{d}\hat{\mu}\,\mathrm{d}\chi\right] \tag{103}$$

and

$$\frac{3}{2}v\int_{-1}^{1}([\hat{\mu}_{\text{eq}}+\chi]^2 - \varepsilon^2[1+R^2(1-\chi^2)])^{1/2}\chi\,\mathrm{d}\chi = 1, \tag{104}$$

$$\hat{\mu}_{\text{wb}} = 1+\varepsilon, \tag{105}$$

where, using (89),

$$a = \frac{3n_{\text{ion}}\gamma^2 v}{4\pi R^2\alpha}, \tag{106}$$

$$\varepsilon = \frac{\gamma}{a} = \frac{4\pi R^2\alpha}{3n_{\text{ion}}\gamma v}. \tag{107}$$

Thus, it follows $\varepsilon \to 0$ as $v \to 1$ and we determine an asymptotic approximation for $E_{\max}$ in ε as $\varepsilon \to 0$.

Expansion in ε of the integrand in (103) yields

$$\begin{aligned}([\hat{\mu}+\chi]^2 - \varepsilon^2[1+R^2(1-\chi^2)])^{1/2} \\ = \hat{\mu}+\chi - \frac{1+R^2(1-\chi^2)}{2(\hat{\mu}+\chi)}\varepsilon^2 + \sum_{n=2}^{\infty} c_n \frac{(1+R^2(1-\chi^2))^n}{(\hat{\mu}+\chi)^{2n-1}}\varepsilon^{2n},\end{aligned} \tag{108}$$

where the c_n are numerical constants. Using (108), the integral over $\hat{\mu}$ in (103) leads to a summand proportional to

$$f_n = \int_{-1}^{1}\left[\frac{(1+R^2(1-\chi^2))^n}{(\hat{\mu}_{\text{eq}}+\chi)^{2n-2}} - \frac{(1+R^2(1-\chi^2))^n}{(1+\varepsilon+\chi)^{2n-2}}\right]\chi\,\mathrm{d}\chi, \quad n \geqslant 2, \tag{109}$$

where (105) has been used.

Inspection of (104) suggests an approximation for $\hat{\mu}_{\text{eq}}(\varepsilon)$ of the form

$$\hat{\mu}_{\text{eq}}(\varepsilon) = h(\varepsilon^2) = h(0) + h'(0)\varepsilon^2 + \mathcal{O}(\varepsilon^4) \quad (\varepsilon \to 0). \tag{110}$$

Using (107), it follows

$$v = \frac{1}{\sqrt{1+\varepsilon^2 b^2}} = 1 - \frac{1}{2}\varepsilon^2 b^2 + \mathcal{O}(\varepsilon^4) \quad (\varepsilon \to 0), \tag{111}$$

$$b = \frac{3n_{\text{ion}}}{4\pi R^2\alpha} = \frac{a}{\gamma^2 v} \tag{112}$$

and (104) leads to

$$-\frac{3}{2}\int_{-1}^{1}\frac{1+R^2(1-\chi^2)}{\hat{\mu}_{\text{eq}}(0)+\chi}\chi\,\mathrm{d}\chi = b^2. \tag{113}$$

Thus, $\hat{\mu}_{\rm eq}(0)$ may be approximated as

$$\hat{\mu}_{\rm eq}(0) = \frac{1}{b}\sqrt{1+\frac{2R^2}{5}} + \mathcal{O}(1) \quad (b \to 0). \tag{114}$$

Repeated integration by parts in (109) leads to

$$f_n = \mathcal{O}(\varepsilon^{3-2n}) \qquad (\varepsilon \to 0), \qquad n \geqslant 2, \tag{115}$$

and we obtain the asymptotic approximation

$$\begin{aligned}
&\int_{-1}^{1}\int_{1+\varepsilon}^{\hat{\mu}_{\rm eq}} ([\hat{\mu}+\chi]^2 - \varepsilon^2[1+R^2(1-\chi^2)])^{1/2}\chi \,\mathrm{d}\chi \,\mathrm{d}\hat{\mu} \\
&\quad = \frac{2}{3}(\hat{\mu}_{\rm eq}-\hat{\mu}_{\rm wb}) - \frac{1}{2}\varepsilon^2\int_{-1}^{1}[1+R^2(1-\chi^2)]\ln\left(\frac{\hat{\mu}_{\rm eq}+\chi}{\hat{\mu}_{\rm wb}+\chi}\right)\chi\,\mathrm{d}\chi \\
&\quad\quad + \mathcal{O}(\varepsilon^3) \quad (\varepsilon \to 0) \\
&\quad = \frac{2}{3}(\hat{\mu}_{\rm eq}-\hat{\mu}_{\rm wb}) - \frac{1}{2}\varepsilon^2\int_{-1}^{1}[1+R^2(1-\chi^2)]\ln\left(\frac{\hat{\mu}_{\rm eq}(0)+\chi}{1+\chi}\right)\chi\,\mathrm{d}\chi \\
&\quad\quad + \mathcal{O}(\varepsilon^3\ln\varepsilon) \quad (\varepsilon \to 0).
\end{aligned} \tag{116}$$

Thus,

$$\begin{aligned}
\frac{E_{\rm max}^2}{a} &= mn_{\rm ion}\varepsilon^2\left\{b^2(1-\hat{\mu}_{\rm eq}(0)) + \frac{3}{2}\int_{-1}^{1}[1+R^2(1-\chi^2)]\ln\left(\frac{1+\chi}{\hat{\mu}_{\rm eq}(0)+\chi}\right)\chi\,\mathrm{d}\chi\right\} \\
&\quad + \mathcal{O}(\varepsilon^3\ln\varepsilon) \qquad (\varepsilon \to 0),
\end{aligned} \tag{117}$$

and retaining lowest order terms in ε, b, R yields

$$\begin{aligned}
E_{\rm max}^2 &\approx \frac{3}{2}mn_{\rm ion}a\varepsilon^2\int_{-1}^{1}[1+R^2(1-\chi^2)]\ln(1+\chi)\chi\,\mathrm{d}\chi, \\
&= 2\pi\alpha m R^2\left(1+\frac{1}{3}R^2\right) \\
&\approx \frac{3}{2}mn_{\rm ion}\frac{1}{b},
\end{aligned} \tag{118}$$

where (112) has been used to eliminate αR^2.

Numerical validity of the above approximation is supported by figure 4. The solid curves are obtained by numerically integrating (103)–(105) and the dashed lines are obtained using (118). It is clear that (118) yields a good approximation to $E_{\rm max}$ for large γ.

In order to compare (118) with expressions for $E_{\rm max}$ obtained elsewhere [10–12], it is useful to express (118) as a function of effective temperature. The electron proper number density is $n = n_{\rm ion}$ when $\mu = \mu_{\rm eq}$ and we eliminate b in favour of an effective longitudinal temperature $T_{\|\rm eq}$ defined as

$$T_{\|\rm eq} = \frac{1}{k_B\, n_{\rm ion}}p_{\|\rm eq}, \tag{119}$$

where k_B is Boltzmann's constant and $p_{\|\rm eq}$ is the longitudinal pressure associated with the oscillator equilibrium $\mu = \mu_{\rm eq}$. The longitudinal pressure is $p_{\|\rm eq} = \mathcal{T}_{\rm eq}^{33}$ where the stress–energy–momentum tensor $\mathcal{T}_{\rm eq}$ has components

$$\mathcal{T}_{\rm eq}^{ab} = m\alpha\int_{\mathcal{W}_{\rm eq}}\dot{x}^a\dot{x}^b\iota_X\#1 \tag{120}$$

with $\mathcal{W}_{\rm eq}$ the support of the waterbag distribution $\mu = \mu_{\rm eq}$ (the choice of fibre is unimportant as the distribution associated with $\mu_{\rm eq}$ is independent of ζ).

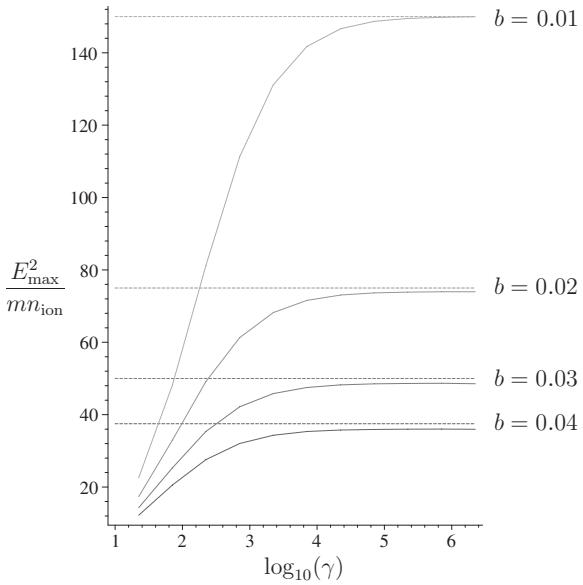

Figure 4. $E^2_{\max}/(mn_{\text{ion}})$ versus $\log_{10}(\gamma)$ for $R = 0.2$ and $b \in \{0.01, 0.02, 0.03, 0.04\}$. The dashed lines are the approximation (118) and the solid curves are obtained by numerically integrating (103)–(105).

Since

$$\frac{\dot{x}^{32}\,\mathrm{d}\dot{x}^1 \wedge \mathrm{d}\dot{x}^2 \wedge \mathrm{d}\dot{x}^3}{\sqrt{\beta^2 + \dot{x}^{32}}} = \mathrm{d}\left\{\left[\frac{1}{2}\dot{x}^3\sqrt{\beta^2 + \dot{x}^{32}} - \frac{1}{2}\beta^2 \sinh^{-1}\left(\frac{\dot{x}^3}{\beta}\right)\right]\mathrm{d}\dot{x}^1 \wedge \mathrm{d}\dot{x}^2\right\} \tag{121}$$

where $\dot{x}^{12} \equiv (\dot{x}^1)^2$, $\dot{x}^{22} \equiv (\dot{x}^2)^2$, $\dot{x}^{32} \equiv (\dot{x}^3)^2$ and $\beta \equiv \sqrt{1 + \dot{x}^{12} + \dot{x}^{22}}$, using (120) and Stokes' theorem on forms [26], it follows

$$\mathcal{T}^{33}_{\text{eq}} = m\alpha \int_{\partial\mathcal{W}_{\text{eq}}} \left[\frac{1}{2}\dot{x}^3\sqrt{\beta^2 + \dot{x}^{32}} - \frac{1}{2}\beta^2 \sinh^{-1}\left(\frac{\dot{x}^3}{\beta}\right)\right]\mathrm{d}\dot{x}^1 \wedge \mathrm{d}\dot{x}^2. \tag{122}$$

Using (82) and (83), components of the oscillator equilibrium waterbag $\dot{x}^a = V^a_{\xi\,\text{eq}}$ are

$$\dot{x}^0 = \mu_{\text{eq}} - a\cos(\xi^1) - v\sqrt{[\mu_{\text{eq}} - a\cos(\xi^1)]^2 - \gamma^2[1 + R^2\sin^2(\xi^1)]}, \tag{123}$$

$$\dot{x}^1 = R\sin(\xi^1)\cos(\xi^2), \tag{124}$$

$$\dot{x}^2 = R\sin(\xi^1)\sin(\xi^2), \tag{125}$$

$$\dot{x}^3 = v[\mu_{\text{eq}} - a\cos(\xi^1)] - \sqrt{[\mu_{\text{eq}} - a\cos(\xi^1)]^2 - \gamma^2[1 + R^2\sin^2(\xi^1)]} \tag{126}$$

and it follows

$$\begin{aligned}\frac{\dot{x}^3}{a} &= v[\hat{\mu}_{\text{eq}} - \cos(\xi^1)] - \sqrt{[\hat{\mu}_{\text{eq}} - \cos(\xi^1)]^2 - \varepsilon^2[1 + R^2\sin^2(\xi^1)]} \\ &\approx \left(-\frac{1}{2}b^2[\hat{\mu}_{\text{eq}}(0) - \cos(\xi^1)] + \frac{1}{2[\hat{\mu}_{\text{eq}}(0) - \cos(\xi^1)]}\right)\varepsilon^2\end{aligned} \tag{127}$$

to lowest order in ε and R. Using (114) and (127), it follows

$$\frac{\dot{x}^3}{a} \approx \varepsilon^2 b^2 \cos(\xi^1) \tag{128}$$

to lowest order in ε, b and R. Furthermore, (107) and (112) yield $a\varepsilon^2 b^2 = b/v \approx b$ and so

$$\dot{x}^3 \approx b \cos(\xi^1) \tag{129}$$

to lowest order in ε, b and R. Hence,

$$\frac{\dot{x}^3}{2}\sqrt{\beta^2 + \dot{x}^{32}} - \frac{1}{2}\beta^2 \sinh^{-1}\left(\frac{\dot{x}^3}{\beta}\right) \approx \frac{1}{3} b^3 \cos^3(\xi^1) \tag{130}$$

to lowest order in ε, b and R and (122) yields

$$\begin{aligned} p_{\|\mathrm{eq}} &\approx \frac{4\pi m \alpha R^2 b^3}{15} \\ &= \frac{1}{5} m n_{\mathrm{ion}} b^2. \end{aligned} \tag{131}$$

Equations (118), (119) and (131) yield

$$E_{\max}^2 \approx \frac{m^2 \omega_p^2 c^2}{q^2}\left(\frac{9mc^2}{20 k_B T_{\|\mathrm{eq}}}\right)^{1/2}, \quad \varepsilon, b, R \ll 1, \tag{132}$$

where $\omega_p = \sqrt{n_{\mathrm{ion}} q^2/(m\varepsilon_0)}$ is the plasma frequency and the speed of light c and permittivity of the vacuum ε_0 have been restored.

5. Conclusion

Equations (81) and (132) indicate that waterbags over two-dimensional spacetime and four-dimensional spacetime can behave quite differently. Equation (132) is independent of γ but (81) diverges as $\gamma \to \infty$, and this difference in behaviour arises because the logarithmic singularity in the integrand in (118) is integrable. Alternatively, one may attribute this disagreement to the different algebraic relationships between the electron proper number density (the metric norm of the first velocity moment of f) and components of the electron stress–energy–momentum tensor (proportional to the second velocity moment of f) associated with waterbags over two-dimensional spacetime and four-dimensional spacetime. Moreover, the $T_{\|\mathrm{eq}}^{-1/4}$ behaviour of the asymptotic form of $E_{\max}$ for $k_B T_{\|\mathrm{eq}} \ll mc^2$ is very similar to the results of SES [12] and others [11] in the limit $v \to c$.

Direct comparison of our results and those of SES follows by setting the transverse vector potential $\boldsymbol{A}_\perp$ to zero in the SES model, thereby neglecting the overlap of the electromagnetic field of the driver (laser pulse or particle bunch) and the wave. The approach followed by SES begins with covariant field equations, induced from the Vlasov equation, that couple the zeroth-, first- and second-order centred moments (in $\dot{x}^a$) of the one-particle distribution f with the electromagnetic field. SES then assume that the one-particle distribution f (restricted by pull-back to the unit hyperboloid) may be approximated as[6] $f \simeq h(x^3 - vx^0, \dot{x}^3)\delta(\dot{x}^1)\delta(\dot{x}^2)$ where δ is the Dirac delta function. A covariant measure of the total thermal spread is given by the magnitude ϵ^2 of the ratio of the trace of the second-order centred moment and the zeroth moment. SES assume that the third-order centred moment is $\mathcal{O}(\epsilon^3)$ and can be neglected relative to lower order moments.

One could develop a similar argument to that given by SES based on moments of a prescribed three-dimensional waterbag with narrow velocity spread, rather than the line

[6] We have changed the notation used by SES to avoid conflict with our own.

distribution employed by SES. However, nuances in the shape of the waterbag would be lost; for example, we would not know that merely the tip of the waterbag grazes the wave's phase velocity (see figure 3) during the maximum amplitude oscillation. This could be important because, as noted earlier, longitudinal wave-breaking is associated with the trapping of considerable numbers of particles in the wave (see [15] for a discussion), and our present model neglects trapped particles. We aim to develop the present work to include the effects of trapped particles, and to extend our calculations beyond the quasi-static approximation.

In conclusion, we have shown that it is possible to construct three-dimensional waterbag distributions that lead to a maximum electric field amplitude whose asymptotic behaviour is similar to that of the SES model as $v \to c$ (with effective temperature held fixed in the limit $v \to c$).

Acknowledgments

We thank RMGM Trines for useful discussions and thank the referees for their helpful comments. We acknowledge EPSRC for financial support.

References

[1] Tajima T and Dawson J M 1979 *Phys. Rev. Lett.* **43** 267
[2] Chen P *et al* 1985 *Phys. Rev. Lett.* **54** 693
[3] Malka V *et al* 2008 *Nat. Phys.* **4** 447
[4] Caldwell A *et al* 2009 *Nat. Phys.* **5** 363
[5] Wuensch A 2002 *Proc. EPAC 2002 (Paris)* p 134
[6] Schlenvoigt H P *et al* 2008 *Nat. Phys.* **4** 133
[7] Akhiezer A I and Polovin R V 1956 *Sov. Phys.—JETP* **3** 696
[8] Dawson J M 1959 *Phys. Rev.* **113** 383
[9] Coffey T P 1971 *Phys. Fluids* **14** 1402
[10] Katsouleas T and Mori W B 1988 *Phys. Rev. Lett.* **61** 90
[11] Rosenzweig J B 1988 *Phys. Rev.* A **38** 3634
[12] Schroeder C B, Esarey E and Shadwick B A 2005 *Phys. Rev.* E **72** 055401
[13] Trines R M G M and Norreys P A 2006 *Phys. Plasmas* **13** 123102
[14] Schroeder C B, Esarey E and Shadwick B A 2007 *Phys. Plasmas* **14** 084701
[15] Trines R M G M and Norreys P A 2007 *Phys. Plasmas* **14** 084702
[16] Mangles S P D *et al* 2004 *Nature* **431** 535
[17] Geddes C G R *et al* 2004 *Nature* **431** 538
[18] Faure J *et al* 2004 *Nature* **431** 541
[19] Lu W *et al* 2006 *Phys. Plasmas* **13** 056709
[20] Esirkepov T *et al* 2006 *Phys. Rev. Lett.* **96** 014803
[21] Mori W B and Katsouleas T 1990 *Phys. Scr.* T **30** 127
[22] Burton D A and Noble A 2009 *AIP Conf. Proc.* **1086** 252
[23] Burton D A, Noble A and Wen H 2009 *Nuovo Cimento* C **32** 1
[24] Ehlers J 1971 *Proceedings of the International School of Physics 'Enrico Fermi'* vol 47 (New York and London: Academic) p 1
[25] Burton D A 2003 *Theor. Appl. Mech.* **30** 85
[26] Benn I M and Tucker R W 1987 *An Introduction to Spinors and Geometry with Applications in Physics* (Bristol and New York: Adam Hilger)